

Detecting non-unitary multiorbital superconductivity with Dirac points at finite energies

J. L. Lado^{1,2} and M. Sigrist²

¹*Department of Applied Physics, Aalto University, Espoo, Finland*

²*Institute for Theoretical Physics, ETH Zurich, 8093 Zurich, Switzerland*

(Dated: February 28, 2022)

Determining the symmetry of the order parameter of unconventional superconductors remains a recurrent topic and non-trivial task in the field of strongly correlated electron systems. Here we show that the behavior of Dirac points away from the Fermi energy is a potential tool to unveil the orbital structure of a superconducting state. In particular, we show that gap openings in such Dirac crossings are a signature of non-unitary multiorbital superconducting order. Consequently, also spectral features at higher energy can help us to identify broken symmetries of superconducting phases and the orbital structure of non-unitary states. Our results show how angle-resolved photo-emission spectroscopy measurements can be used to detect non-unitary multiorbital superconductivity.

I. INTRODUCTION

Superconductors belong to the most intriguing states of matter, through their rich phenomenology, the range of underlying physical mechanisms, their different solid-state realizations and ultimately, their potential technological applications. Nowadays we label superconductors as conventional or unconventional depending on the symmetry properties of their Cooper pairing states. Conventional includes all superconductors realizing Cooper pairs of highest symmetry, whose wave function is essentially structureless and spin-singlet. In contrast, the term unconventional encompasses all other cases, in particular, those with superconducting order parameters which violate additional symmetries such as lattice, time-reversal or orbital symmetries, or form topologically non-trivial phases¹⁻³. Strongly correlated electron systems provide an especially fertile ground for the unconventional superconductivity as they offer a large variety of low-energy fluctuations to favoring different Cooper pairing channels^{4,5}.

While the major concepts for unconventional superconductivity are based on single-band descriptions, multi-orbital features increase complexity. For many of the recently found superconductors a multi-orbital approach seems mandatory to understand the intricate relation of the superconducting phase with the orbital degrees of freedom and to yield sensible mechanisms for pairing^{6,7}. Very recent experiments on Fe-chalcogenides⁷ may show some intriguing aspect of orbital selectivity of the superconducting phase⁷. In angle-resolved photoemission spectroscopy (ARPES) a conspicuous gap opening of Dirac points rather far away from the Fermi energy has been observed and interpreted in terms of spontaneous time-reversal symmetry breaking stemming from a spontaneous magnetization associated to the superconducting state^{8,9}. Motivated by this finding, we would like to address this feature of the remote Dirac points¹⁰ from a general viewpoint and show that this peculiarity may give interesting insights into the multi-orbital nature of the superconducting phase on a general setup.

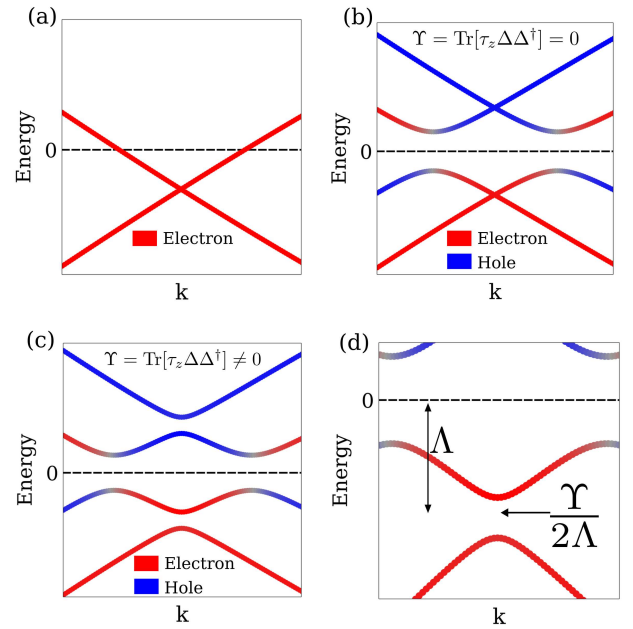


FIG. 1. (a) Sketch of the normal state band structure, featuring a Dirac crossing away from the chemical potential. (b) Sketch of the band structure in a unitary superconducting state, showing that the Dirac point stays closed. In stark comparison, the onset of a non-unitary superconducting state opens up the Dirac point away from the chemical potential as shown in panel (c). The magnitude of the gap opening at the Dirac crossing depends on the non-unitarity Υ and the distance to the chemical potential as shown in panel (d).

Here we demonstrate that a gap opening in a remote Dirac point upon entering a superconducting state indicates the realization of non-unitarity of Cooper pairing states in orbital space, due to specific forms of orbital selective pairing. The basic phenomenology is depicted in Fig.1, showing in Fig.1 (a) the normal state spectrum with a Dirac point remote from the Fermi level. After extending the electronic states by holes to the Nambu space, we obtain the standard spectrum of

a superconductor with a gap around the Fermi energy (Fig.1(b,c)). A unitary pairing state leaves the Dirac points untouched (Fig.1(b)), while for non-unitary phases these Dirac points disappear by a gap opening (Fig.1(c)). In the enlarged panel Fig. 1(d) we indicate that the size of the gap is controlled by Υ , a measure for non-unitarity, as we define below. We note that the physical mechanism leading to the superconducting state can be of various kind, including charge or antiferromagnetic fluctuation, yet its nature will not affect our analysis. The paper is organized as follows: in Sec. II we show an analysis based on a minimal Dirac equation, in Sec. III we show how our mechanism applies to a real space model, in Sec. IV we present how the non-unitarity creates topological interface excitations and in Sec. V we summarize our conclusions.

II. NON-UNITARITY IN A CONTINUUM MODEL

For the theoretical approach to this problem, we first consider a generic two-orbital system with a two-dimensional Bloch Hamiltonian hosting a Dirac crossing¹¹ away from the Fermi level (Fig. 1(a)). We focus on the region near the Dirac points of a two-dimensional band structure using a $\mathbf{k} \cdot \mathbf{p}$ description with the spinor basis $\psi_{\mathbf{k}}^{\dagger} = (c_{\alpha,\mathbf{k}}^{\dagger}, c_{\beta,\mathbf{k}}^{\dagger})$, where $c_{\alpha,\mathbf{k}}^{\dagger}$ and $c_{\beta,\mathbf{k}}^{\dagger}$ denote electronic creation operators of Bloch states with momentum \mathbf{k} and the indices α, β label the two orbitals, including also the spin degrees of freedom. Then the effective Hamiltonian is written as $\mathcal{H}_0^{DP}(\mathbf{k}) = \psi_{\mathbf{k}}^{\dagger} H_0^{DP}(\mathbf{k}) \psi_{\mathbf{k}}$, where $H_0^{DP}(\mathbf{k})$ is a 2×2 matrix of the form

$$H_0^{DP}(\mathbf{k}) = -\Lambda\tau_0 + \tau_x k_x + \tau_y k_y. \quad (1)$$

The absence of the Pauli matrix τ_z in Eq. 1 guarantees the existence of a Dirac crossing at the energy $-\Lambda$.

We now turn to the superconducting state. For simplicity, we consider here pairing of electrons between time-reversal Kramers partners, which includes conventional superconducting states. Note that other channels such as spin triplet pairing states could be treated in an analogous way. Thus, we extend the Hamiltonian to $\mathcal{H}_{BdG}(\mathbf{k}) = \mathcal{H}_0^{DP}(\mathbf{k}) + \frac{1}{2} \sum_{i,j \in \alpha, \beta} c_{i,\mathbf{k}}^{\dagger} c_{j,-\mathbf{k}}^{\dagger} \Delta_{ij}(\mathbf{k}) + h.c.$, where $\bar{\alpha}, \bar{\beta}$ label the Kramers time-reversal partners of α, β in orbital and spin space. We write the 2×2 gap matrix as

$$\Delta(\mathbf{k}) = \begin{pmatrix} \Delta_{\alpha\alpha}(\mathbf{k}) & \Delta_{\alpha\beta}(\mathbf{k}) \\ \Delta_{\beta\alpha}(\mathbf{k}) & \Delta_{\beta\beta}(\mathbf{k}) \end{pmatrix} \quad (2)$$

with $\Delta_{\alpha\alpha}(\mathbf{k}) = \langle c_{\alpha,\mathbf{k}} c_{\bar{\alpha},-\mathbf{k}} \rangle$, $\Delta_{\alpha\beta}(\mathbf{k}) = \langle c_{\alpha,\mathbf{k}} c_{\bar{\beta},-\mathbf{k}} \rangle$, $\Delta_{\beta\alpha}(\mathbf{k}) = \langle c_{\beta,\mathbf{k}} c_{\bar{\alpha},-\mathbf{k}} \rangle$, $\Delta_{\beta\beta}(\mathbf{k}) = \langle c_{\beta,\mathbf{k}} c_{\bar{\beta},-\mathbf{k}} \rangle$. For systems where s_z is a good quantum number, the indices are $\alpha \equiv (\alpha_0, \uparrow)$ and $\bar{\alpha} \equiv (\alpha_0, \downarrow)$ with α_0 the orbital label, such that $\Delta(\mathbf{k}) \equiv \Delta^{\uparrow\downarrow}(\mathbf{k})$ describes opposite spin

pairing. For concreteness, we continue now with this orbital spin labeling, although more general Kramers pairs yield the same behavior. With the Nambu spinor $\Psi_{\mathbf{k}}^{\dagger} = (c_{\alpha_0,\uparrow,\mathbf{k}}^{\dagger}, c_{\beta_0,\uparrow,\mathbf{k}}^{\dagger}, c_{\alpha_0,\downarrow,-\mathbf{k}}, c_{\beta_0,\downarrow,-\mathbf{k}})$, the Bogoliubov-de-Gennes (BdG) Hamiltonian H_{BdG} takes the form $\mathcal{H}_{BdG} = \frac{1}{2} \Psi_{\mathbf{k}}^{\dagger} H_{BdG}(\mathbf{k}) \Psi_{\mathbf{k}} + h.c.$, where $H_{BdG}(\mathbf{k})$ is the following 4×4 matrix

$$H_{BdG}(\mathbf{k}) = \begin{pmatrix} H_0^{DP}(\mathbf{k}) & \Delta(\mathbf{k}) \\ \Delta(\mathbf{k}) & -H_0^{DP}(-\mathbf{k}) \end{pmatrix} \quad (3)$$

Using this Hamiltonian, we now derive the corrections induced by the Cooper pairing at the Dirac point of Eq. 1. A Schrieffer-Wolff transformation equivalent to second order perturbation theory leads to the effective Hamiltonian around the Dirac point $\mathbf{k} = \mathbf{K}$ of the form

$$H^{DP} = H_0^{DP} + \frac{\Delta\Delta^{\dagger}}{2\Lambda} \quad (4)$$

with $\Delta \equiv \Delta(\mathbf{K})$, valid in the limit $|\Lambda| \gg \max(|\Delta|)$.

As a 2×2 matrix, the correction to the Dirac Hamiltonian in Eq. 4 can be decomposed into the identity \mathcal{I} and Pauli matrices τ_i as $\frac{\Delta\Delta^{\dagger}}{2\Lambda} = \gamma_0 \mathcal{I} + \gamma_x \tau_x + \gamma_y \tau_y + \gamma_z \tau_z$ with $\gamma_0, \gamma_x, \gamma_y, \gamma_z$ real numbers, where $\gamma_x = \gamma_y = \gamma_z = 0$ defines a unitary pairing state. Generally, this yields an effective Hamiltonian around the original Dirac point that can be again written in terms the identity \mathcal{I} and Pauli matrices τ_i as,

$$H^{DP} = -\bar{\Lambda}\tau_0 + \bar{p}_x \tau_x + \bar{p}_y \tau_y + \gamma_z \tau_z \quad (5)$$

with $\bar{\Lambda} = \Lambda - \gamma_0$, $\bar{p}_x = p_x + \gamma_x$ and $\bar{p}_y = p_y + \gamma_y$. This highlights that a non-unitary superconducting term modifies the Dirac crossing away from the chemical potential. As a result, the existence of non-unitary pairing can be generically observed by analyzing the behavior of Dirac point in the superconducting state. For non-vanishing $\gamma_x \neq 0$ or $\gamma_y \neq 0$, the onset of superconductivity will shift the Dirac point in reciprocal space. But more importantly, for $\gamma_z \neq 0$ in Eq. 5 a gap opens at the Dirac point. Generally, the condition to open a gap at the Dirac point can be written in terms of the non-unitarity parameter Υ of the gap matrix as $\Upsilon = \sum_{\nu=\alpha,\beta} [\Delta_{\alpha,\nu} \Delta_{\alpha,\nu}^* - \Delta_{\beta,\nu} \Delta_{\beta,\nu}^*]$, which in matrix form reads

$$\Upsilon = \text{Tr}[\tau_z \Delta \Delta^{\dagger}] \neq 0 \quad (6)$$

yielding $\gamma_z = \Upsilon/4\Lambda$ in Eq. 5. We point out that a similar analysis could be carried out both for one-dimensional and three-dimensional systems described by a 2×2 Dirac equation. However, in the three dimensional case, a gap can not be induced in the 2×2 Dirac Hamiltonian, as any correction will only create a momentum shift.

We examine now a few examples based on this criterion. We start with the unitary states. First the intra-orbital state given by $\Delta(\mathbf{k}) = \Delta_0 \tau_0 f(\mathbf{k})$ which for

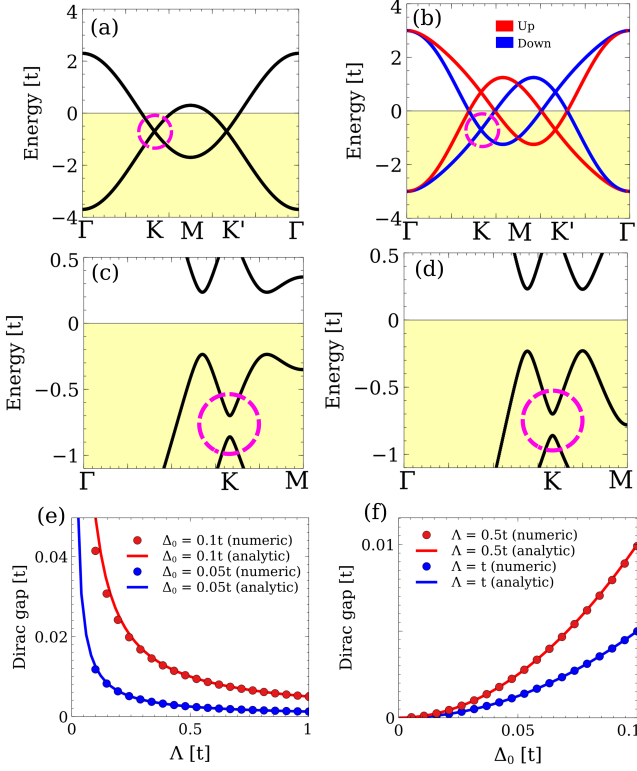


FIG. 2. Normal state band structure (a,b) for a Dirac band system in the normal state, showing Dirac crossings away from the chemical potential. Panel (a) shows a doped honeycomb lattice without spin orbit-coupling, whereas panel (b) shows a half filled honeycomb system with non-centrosymmetric spin-orbit coupling (b). Panel (c) shows the BdG spectra in the presence of non-unitary superconducting term for (a), and panel (d) the analogous spectra for the case (b). In both scenarios, it is observed that the non-unitary superconducting state drives a gap opening at the Dirac point. Panels (e,f) show a comparison between the numeric and analytic results for Dirac gap opening. In particular, panel (e) shows the Dirac gap as a function of the distance to the chemical potential Λ (e), and panel (f) the Dirac gap as a function of the non-unitary superconducting term. We took $\Lambda_1 = 0.7t$ and $\Lambda_2 = 0$ for (a,c), $\Lambda_1 = 0.0$ and $\Lambda_2 = 0.7t$ for (b,d), $\Lambda_2 = 0$ for panels (e,f) and $\Delta_0 = 0.71\Lambda$ for (c,d).

$f(\mathbf{k}) = \text{const.}$ corresponds to a conventional superconductor. This leads obviously to $\Upsilon = 0$. The same is true of an inter-orbital pairing state like $\Delta(\mathbf{k}) = \Delta_0 \tau_x f(\mathbf{k})$. A linear combination of these two states is non-unitary with $\Upsilon = 0$, and leads to a shift of the Dirac points.

A straightforward case opening a gap is the intra-orbital pairing state $\Delta(\mathbf{k}) = \Delta_0 f(\mathbf{k}) \begin{pmatrix} 1 & 0 \\ 0 & 0 \end{pmatrix} = \Delta_0 f(\mathbf{k})(\tau_0 + \tau_z)/2$, which corresponds to pairing restricted to one orbital only and leads to $\Upsilon \neq 0$. Such a state breaks orbital symmetry, and it is expected to appear close to a quantum critical point to an orbital ordered instability. An exemplary non-unitary

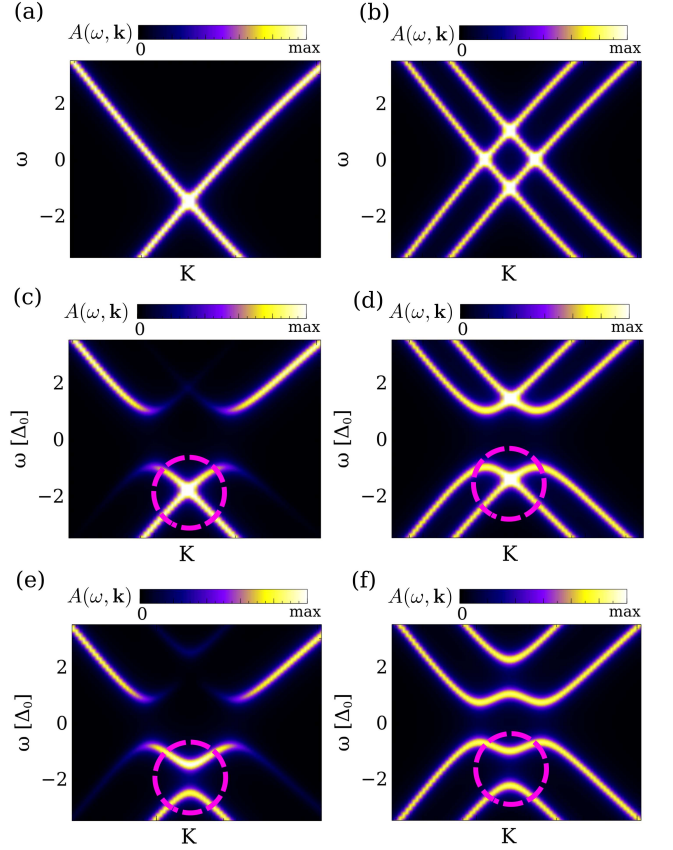


FIG. 3. Electron spectral function $A(\omega, \mathbf{k})$ for a system with a Dirac point away from the chemical potential due to doping (a,c,e) and due to spin-orbit coupling (b,d,f). Panels (a,b) show the spectral function in the normal state, depicting a Dirac crossing away from the chemical potential. In the presence of unitary orbital superconductivity, a gap opens up at the chemical potential, but not at the Dirac crossings (c,d). In contrast, in the presence of a non-unitary superconducting state a gap opens up at the Dirac crossing (e,f). We took $\Lambda_1 = 1.5\Delta_0$ and $\Lambda_2 = 0$ in (a,c,e), $\Lambda_1 = 0$ and $\Lambda_2 = \Delta_0$ in (b,d,f).

state for inter-orbital pairing is $\Delta = \Delta_0 f(\mathbf{k}) \begin{pmatrix} 0 & 1 \\ 0 & 0 \end{pmatrix} = \Delta_0 f(\mathbf{k})(\tau_x + i\tau_y)/2$, which shows spontaneous time-reversal symmetry breaking in orbital space and realizes an antiferromagnetic superconducting state breaking spin rotational symmetry. This state is expected to appear close to a quantum phase transition to an antiferromagnetic instability. We finally emphasize that in the previous description we have not assumed any momentum space structure of the superconducting state, and as a result this argument can be applied to arbitrary momentum superconducting structures.

III. NON-UNITARITY IN A REAL SPACE MODEL

We now illustrate this analysis on a specific tight-binding model for the honeycomb lattice. The role of orbitals is now played by the two sublattices. The Hamiltonian has the form

$$\begin{aligned} \mathcal{H}_{TB} = & t \sum_{\langle ij \rangle, s} c_{i,s}^\dagger c_{j,s} + \Lambda_1 \sum_{i,s} c_{i,s}^\dagger c_{i,s} \\ & + \Lambda_2 \frac{i}{3\sqrt{3}} \sum_{\langle\langle ij \rangle\rangle, s, s'} \nu_{ij} \sigma_z^{ss'} \tau_z^{ij} c_{i,s}^\dagger c_{j,s'} \\ & + \sum_i (\Delta_i^{\uparrow\downarrow} c_{i,\uparrow} c_{i,\downarrow} + h.c.) \end{aligned} \quad (7)$$

with $c_{i,s}^\dagger, c_{i,s}$ are the creation/annihilation operators of electrons on the site i with spin s , $\langle \rangle$ denotes the summation over nearest neighbors, $\langle\langle \rangle\rangle$ over next-nearest neighbors, σ^z is the corresponding spin Pauli matrix and $\nu_{ij} = \pm 1$ for clockwise/anticlockwise hopping within each hexagonal plaquette, whereby an additional sign difference enters through the orbital Pauli matrix τ_z , giving the opposite sign for the two sublattices. Note that the Λ_2 term describes the non-centrosymmetric spin-orbit coupling for next-nearest neighbor hopping, which induces a momentum-dependent spin-splitting in the band structure with shifted Dirac cones^{12,13}. The Λ_1 term introduces merely the chemical potential which is finite and negative for the electron-doped system. Finally, $\Delta_i^{\uparrow\downarrow}$ controls the amplitude of the onsite pairing state, yielding an intra-orbital pairing. We will use here the simplest spin singlet s-wave superconducting pairing to highlight the impact of a non-trivial orbital structure even for a topologically trivial superconducting state. Other superconducting momentum structures could be studied analogously.^{14,15}

The Hamiltonian Eq. 7 has two simple limiting cases. First, for $\Lambda_1 \neq 0$ and $\Lambda_2 = 0$, the band structure shows two Dirac points below the Fermi level, realizing a doped honeycomb lattice (Fig. 2(a)). Second, with $\Lambda_1 = 0$ and $\Lambda_2 \neq 0$ the system is half-filled, but the Dirac cones are spin split due to the non-centrosymmetric spin-orbit coupling, and there are again Dirac points away from the Fermi energy (Fig. 2(b)). In the generic case, $\Lambda_1 \neq 0$ and $\Lambda_2 \neq 0$, Dirac crossings will appear at energies $\Lambda = \Lambda_1 \pm \Lambda_2$.

Now we introduce the non-unitary pairing state $\Delta = \Delta_0(\tau_0 + \tau_z)/2$, which corresponds to onsite pairing on one of the two sublattices only. For both limiting cases, the Dirac point remote from the Fermi energy develops a gap as seen in Fig. 2(c,d). Moreover, we compute the magnitude of this gap as function of $\Lambda = \Lambda_1$ and Δ_0 and compare this with our result for $\Upsilon/2\Lambda$ of Eq.(6) demonstrating very good agreement as long as the condition $|\Lambda| \gg |\Delta_0|$ is satisfied (Fig. 2(e,f)). Note that this pairing state is a so-called pair density wave state

and corresponds to a spontaneous sublattice symmetry breaking. It would be accompanied by a charge density difference on the two sublattices and is stabilized in systems where superconductivity appears close to quantum phase transition to a charge density wave instability.

We now discuss the electron spectra function which is experimentally accessible, for instance, by ARPES. This can be computed through,

$$A(\omega, \mathbf{k}) = -\frac{1}{\pi} \text{Im}[\text{Tr}[P_e(\omega - H(\mathbf{k}) + i0^+)^{-1}]] \quad (8)$$

with $H(\mathbf{k})$ as the corresponding BdG Hamiltonian in the Nambu representation and P_e the projection operator on the electron sector. The quantity $A(\omega, \mathbf{k})$ would be the observable in an ARPES experiment in the superconducting state, as shown in Fig. 3. We consider again the two limiting cases for the Dirac cones shifted below the Fermi energy in Fig. 3(a,c,e) for electron doping and in Fig. 3(b,d,f) for spin-orbit coupling. The spectrum for the normal state spectrum is shown in Fig. 3(a,b), and for superconducting states in Fig. 3(c,d,e,f), both for a unitary (Fig. 3(c,d)) and a non-unitary (Fig. 3(e,f)) superconducting state. The unitary state is given by $\Delta^U = \Delta_0\tau_0$ and the non-unitary one by $\Delta = \Delta_0(\tau_0 + \tau_z)/2$. As anticipated from our discussion above, again a gap opens at the Dirac points below from the Fermi level only if the pairing state is non-unitary. In all cases the superconducting gap at the Fermi energy is fully open.

The real space analysis demonstrates that the mechanism we presented is robust against corrections to the Dirac dispersion such as trigonal warping or electron-hole asymmetry, present in the lattice model but not in the continuum model. As a result, the lattice model demonstrates that our phenomenology is a robust mechanism that will apply even in cases beyond a minimal Dirac equation, highlighting that it will be applicable to dispersions of real compounds. This will be especially important in the next section, when we show the emergence of non-trivial interface excitation on a real-space boundary.

IV. INTERFACE MODES ASSOCIATED TO NON-UNITARITY

Gapped Dirac points are a known source of topological excitations. In the following, we show how these gaps give rise to in-gap excitations at domain walls between superconducting domains, which otherwise lack any spectroscopic signature at the Fermi energy. For this purpose, we now take an interface between two degenerate non-unitary superconducting phases A and B , namely $\Delta_A = \Delta_0(\tau_0 + \tau_z)/2$ and $\Delta_B = \Delta_0(\tau_0 - \tau_z)/2$. We now consider a system with translational invariance along the domain wall, direction \parallel , with Δ_A on the left and Δ_B on the right (see Fig. 4(a)). Here the spectral function at the superconducting domain wall can be obtained by the

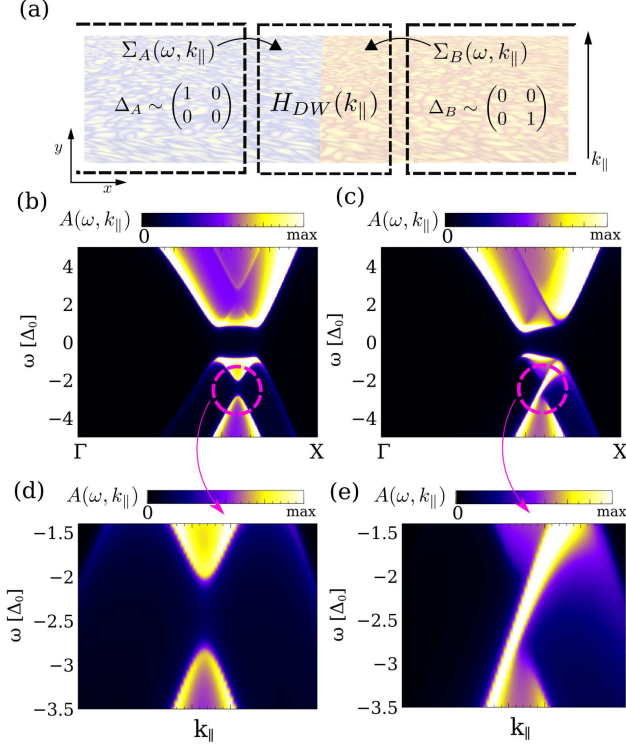


FIG. 4. (a) Sketch of an interface between two superconducting domains with different non-unitary orders Δ_A and Δ_B . Panels (b,c) show the bulk spectral function of the superconductor in the absence of a superconducting domain wall, showing the gap opening in the buried Dirac point (b,d). In contrast, at the interface between the two superconducting domains, a chiral excitation appears inside the Dirac opening as shown in (c,e). We took $\Lambda = 1.5\Delta_0$.

Green's function $G(\omega, k_{\parallel}) = [\omega - H_{DW}(k_{\parallel}) - \Sigma_A(\omega, k_{\parallel}) - \Sigma_B(\omega, k_{\parallel})]^{-1}$ where k_{\parallel} is the momentum parallel to the domain wall, and H_{DW} denotes the local Hamiltonian at the interface, where, for simplicity, we take a sharp transition between the two superconducting gaps. The self-energies $\Sigma_{A,B}(\omega, k_{\parallel})$ are induced by the semi-infinite superconducting regions, which can be exactly computed through a frequency dependent renormalization group algorithm.¹⁶ Then the spectral function at the interface can be computed by $A(\omega, k_{\parallel}) = -\frac{1}{\pi} \text{Im}[\text{Tr}[P_e G(\omega, k_{\parallel})]]$, which gives access to the local excitations. Physically, the system we are computing corresponds to an interface between two semi-infinite superconducting orders with a sharp transition between, yet this procedure can be trivially extended to a smooth transition.

Away from the domain wall, the Dirac point shows a gap in the \mathbf{k} -resolved spectral function (Fig. 4(b,d)). At the domain wall, a chiral state appears inside the gap, corresponding to a chiral Andreev bound state (Fig. 4(c,e)). The origin of such in-gap excitations can be easily rationalized by defining the Chern number associated

to the effective Dirac Hamiltonian Eq. 4,

$$C = \frac{1}{2} \text{sign}(\Upsilon) \text{sign}(\Lambda) \quad (9)$$

Taking $\Delta_0 > 0$ for Δ_A and Δ_B , we obtain $C_A = +1/2$ and $C_B = -1/2$, which from the index theorem implies that a single interface state will appear inside the Dirac gap (Fig. 4(e)).¹⁷ We emphasize that the non-integer nature of the Chern number stems from the fact that the Dirac equation is defined in a non-compact manifold, which is associated with taking a Dirac equation as a low energy approximation. Interestingly, such interface states in the Dirac gap do not create an Andreev bound states within the actual superconducting gap at the Fermi level. This shows that such domain walls are invisible in the actual low-energy spectroscopic gap of the superconductor, but can be observed by targeting Dirac point openings away from the chemical potential. Note that there are no states inside the Dirac opening in a boundary with vacuum,¹⁸ such that only the gap opening at the Dirac points would be visible in ARPES at a surface. We finally mention that the real-space model allows to clearly demonstrate the emergence of interface excitations between the two superconducting domains by exactly computing such a real space interface. This robustly shows that potential corrections to the low energy model do not spoil the topological interface modes, demonstrating that an approximate analysis in terms of a low energy Dirac equation can yield qualitatively faithful results.

V. CONCLUSIONS

To summarize, we have shown that a gap opening at a Dirac point away from the Fermi level is a hallmark of a multiorbital non-unitary state. In particular, our results show that information on the orbital symmetry of the superconducting state could be directly extracted from an ARPES experiment, providing a simple spectroscopic technique to detect unconventional non-unitary superconductivity of this kind. On the one hand, our methodology can be readily applied to iron chalcogenides, where signatures of orbital-selective states have been observed,⁷ and that are known to host remote Dirac crossings in the band structure¹⁹. On the other hand, our results may potentially provide an alternative route to characterize the superconducting state of twisted bilayer graphene,^{20–22} as it hosts Dirac points 10 meV below the Fermi level.^{23–26} Ultimately, our results highlight that ARPES measurements can help to identify the origin of superconductivity in Dirac compounds. Moreover, it may also reveal the presence of an incipient order, such as a charge density wave in our example above, which might be involved in the pairing mechanism due to strong fluctuations.

Acknowledgements: We are grateful to P. Johnson for many helpful discussions on his experimental results.

J.L.L. is grateful for financial support from the ETH Fellowship program and M.S. from the Swiss National Science Foundation through Division II (Grant No. 184739).

-
- ¹ A. J. Leggett, *Rev. Mod. Phys.* **47**, 331 (1975).
 - ² M. Sigrist and K. Ueda, *Rev. Mod. Phys.* **63**, 239 (1991).
 - ³ M. Sato and Y. Ando, *Reports on Progress in Physics* **80**, 076501 (2017).
 - ⁴ C. Pfleiderer, *Rev. Mod. Phys.* **81**, 1551 (2009).
 - ⁵ D. J. Scalapino, *Rev. Mod. Phys.* **84**, 1383 (2012).
 - ⁶ G. R. Stewart, *Rev. Mod. Phys.* **83**, 1589 (2011).
 - ⁷ P. O. Sprau, A. Kostin, A. Kreisel, A. E. Böhrer, V. Taufour, P. C. Canfield, S. Mukherjee, P. J. Hirschfeld, B. M. Andersen, and J. C. S. Davis, *Science* **357**, 75 (2017).
 - ⁸ N. Zaki, G. Gu, A. M. Tsvelik, C. Wu, and P. D. Johnson, *arXiv e-prints*, arXiv:1907.11602 (2019), arXiv:1907.11602 [cond-mat.supr-con].
 - ⁹ L.-H. Hu, P. D. Johnson, and C. Wu, *arXiv e-prints*, arXiv:1906.01754 (2019), arXiv:1906.01754 [cond-mat.supr-con].
 - ¹⁰ L. Komendová, A. V. Balatsky, and A. M. Black-Schaffer, *Phys. Rev. B* **92**, 094517 (2015).
 - ¹¹ T. Wehling, A. Black-Schaffer, and A. Balatsky, *Advances in Physics* **63**, 1 (2014).
 - ¹² F. D. M. Haldane, *Phys. Rev. Lett.* **61**, 2015 (1988).
 - ¹³ C. L. Kane and E. J. Mele, *Phys. Rev. Lett.* **95**, 226801 (2005).
 - ¹⁴ P. M. R. Brydon, D. S. L. Abergel, D. F. Agterberg, and V. M. Yakovenko, *Phys. Rev. X* **9**, 031025 (2019).
 - ¹⁵ P. M. R. Brydon, D. F. Agterberg, H. Menke, and C. Timm, *Phys. Rev. B* **98**, 224509 (2018).
 - ¹⁶ M. P. L. Sancho, J. M. L. Sancho, J. M. L. Sancho, and J. Rubio, *Journal of Physics F: Metal Physics* **15**, 851 (1985).
 - ¹⁷ R. Jackiw and C. Rebbi, *Phys. Rev. D* **13**, 3398 (1976).
 - ¹⁸ A zigzag interface with vacuum will show a flat band of zigzag boundary modes, yet without crossing the gap.
 - ¹⁹ S. Y. Tan, Y. Fang, D. H. Xie, W. Feng, C. H. P. Wen, Q. Song, Q. Y. Chen, W. Zhang, Y. Zhang, L. Z. Luo, B. P. Xie, X. C. Lai, and D. L. Feng, *Phys. Rev. B* **93**, 104513 (2016).
 - ²⁰ Y. Cao, V. Fatemi, S. Fang, K. Watanabe, T. Taniguchi, E. Kaxiras, and P. Jarillo-Herrero, *Nature* **556**, 43 (2018).
 - ²¹ M. Yankowitz, S. Chen, H. Polshyn, Y. Zhang, K. Watanabe, T. Taniguchi, D. Graf, A. F. Young, and C. R. Dean, *Science* **363**, 1059 (2019).
 - ²² X. Lu, P. Stepanov, W. Yang, M. Xie, M. A. Aamir, I. Das, C. Urgell, K. Watanabe, T. Taniguchi, G. Zhang, A. Bachtold, A. H. MacDonald, and D. K. Efetov, *Nature* **574**, 653 (2019).
 - ²³ E. Suárez Morell, J. D. Correa, P. Vargas, M. Pacheco, and Z. Barticevic, *Phys. Rev. B* **82**, 121407 (2010).
 - ²⁴ J. M. B. Lopes dos Santos, N. M. R. Peres, and A. H. Castro Neto, *Phys. Rev. Lett.* **99**, 256802 (2007).
 - ²⁵ R. Bistritzer and A. H. MacDonald, *Proceedings of the National Academy of Sciences* **108**, 12233 (2011).
 - ²⁶ S. L. Tomarken, Y. Cao, A. Demir, K. Watanabe, T. Taniguchi, P. Jarillo-Herrero, and R. C. Ashoori, *Phys. Rev. Lett.* **123**, 046601 (2019).